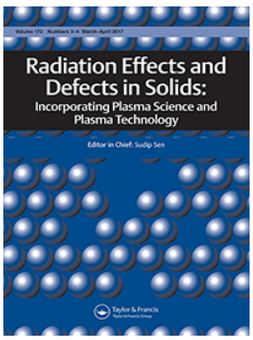

Taylor & Francis
Taylor & Francis Group

Radiation Effects and Defects in Solids
Incorporating Plasma Science and Plasma Technology

ISSN: 1042-0150 (Print) 1029-4953 (Online) Journal homepage: http://www.tandfonline.com/loi/grad20

Effect of 10 MeV electron irradiation on dye-sensitized solar cells

Yunpeng Liu, Xiaobin Tang, Min Liu, Zhiheng Xu, Zhenrong Zhang & Meihua Fang

To cite this article: Yunpeng Liu, Xiaobin Tang, Min Liu, Zhiheng Xu, Zhenrong Zhang & Meihua Fang (2017) Effect of 10 MeV electron irradiation on dye-sensitized solar cells, Radiation Effects and Defects in Solids, 172:3-4, 342-353, DOI: 10.1080/10420150.2017.1320400

To link to this article: http://dx.doi.org/10.1080/10420150.2017.1320400

RADIATION EFFECTS & DEFECTS IN SOLIDS, 2017
VOL. 172, NOS. 3–4, 342–353
https://doi.org/10.1080/10420150.2017.1320400

Taylor & Francis
Taylor & Francis Group

Effect of 10 MeV electron irradiation on dye-sensitized solar cells

Yunpeng Liu[a,b], Xiaobin Tang[a,b], Min Liu[a], Zhiheng Xu[a], Zhenrong Zhang[a] and Meihua Fang[c]

[a]Department of Nuclear Science and Engineering, Nanjing University of Aeronautics and Astronautics, Nanjing, People's Republic of China; [b]Jiangsu Key Laboratory of Material and Technology for Energy Conversion Institutions, Nanjing, People's Republic of China; [c]Department of Space Science and Application, Nanjing University of Aeronautics and Astronautics, Nanjing, People's Republic of China

ABSTRACT

The effect of 10 MeV electrons' irradiation on dye-sensitized solar cells (DSSCs) has been studied in this paper. *J–V* characteristics measurements were carried out in order to investigate the degradation of the cells in electron radiation environments. The short-circuit current (J_{sc}) and maximum power density (P_{max}) of cells decrease significantly after the electron irradiation. When the irradiation dose increases to 10 kGy, the initial maximum power decreases nearly by 50%. The influences of the electron irradiation on FTO, dye sensitizer and anode were studied to investigate the degradation mechanism of DSSC, respectively. The ultraviolet–visible spectra of FTO show that the absorption peaks of dye decrease, resulting in a decline of the FTO transmittance. According to the X-ray diffraction measurement results, it was found that the particle size of nano-crystalline TiO_2 had changed after the electron irradiation. With the help of SEM, the conglomeration of TiO_2 nano-particles appears after the electron irradiation.

ARTICLE HISTORY
Received 3 October 2016
Accepted 10 April 2017

KEYWORDS
Dye-sensitized solar cell (DSSC); electron irradiation effect; irradiation damage; fluorine-doped tin oxide; dye N719; nano-crystalline TiO_2

1. Introduction

Solar cells have come into widespread use for solar energy conversion, particularly for power supplies in orbiting spacecraft, as the orbiting spacecraft suffer space radiations that consist mainly of high energy electrons and protons (*1–3*). These charged particles will cause irradiation damage inside of solar cells, which poses a major threat to the reliability and safety of a spacecraft (*4, 5*).

Dye-sensitized solar cells (DSSCs) have recently received great attention because of their ease of fabrication, cost-effectiveness and environmental friendliness (*6–8*). The maximum efficiency of a dye-sensitized solar cell (DSSC) has already reached 12.3% (*9*). A DSSC is expected to become a potential space solar cell. A DSSC is composed by five parts: fluorine-doped tin oxide (FTO), semiconductor porous thin-film photoelectrode, dye sensitizer, electrolyte and counter electrode. If DSSSs can be applied to radiation environments, such as outer space, some parts of DSSCs may be damaged by particles' irradiation (*10, 11*).

CONTACT Yunpeng Liu liuyp@nuaa.edu.cn

As a result, radiation damage could cause the loss of cell performance. We have studied the variation of dye-sensitized solar cell parameters under γ irradiation, and found that the performance of the DSSC has a significant decline (*12*). However, the electron irradiation damage on the entire DSSC has not been reported so far.

To study the electron irradiation effects on the electrical characteristics of DSSC under illumination, the *J–V* curves of the DSSC were investigated in this paper. The influences of the electron irradiation on FTO, dye sensitizer and anode were studied to investigate the degradation mechanism of DSSC. The results of this research can provide an experimental reference for the study of electron irradiation effects on DSSCs.

2. Experimental preparation and measurement

2.1. The working principle of a DSSC

As illustrated in Figure 1, a typical DSSC is composed by five parts: conducting glass (FTO or indium-tin-oxide), semiconductor porous thin-film photoelectrode, dye sensitizer, electrolyte and counter electrode (*13*). A DSSC differs from conventional semiconductor devices, in which they separate the function of light absorption from charge carrier transport. In the case of *n*-type materials, such as TiO_2, current is generated when a photon absorbed by a dye molecule gives rise to electron injection into the conduction band of the semiconductor. The dye is regenerated by electron transfer from a redox species in solution which is then reduced at the counter electrode. The photovoltage in Figure 1, generated by the cell, corresponds to the difference between the Fermi level in the semiconductor under illumination and the Nernst potential of the redox couple in the electrolyte (*7*).

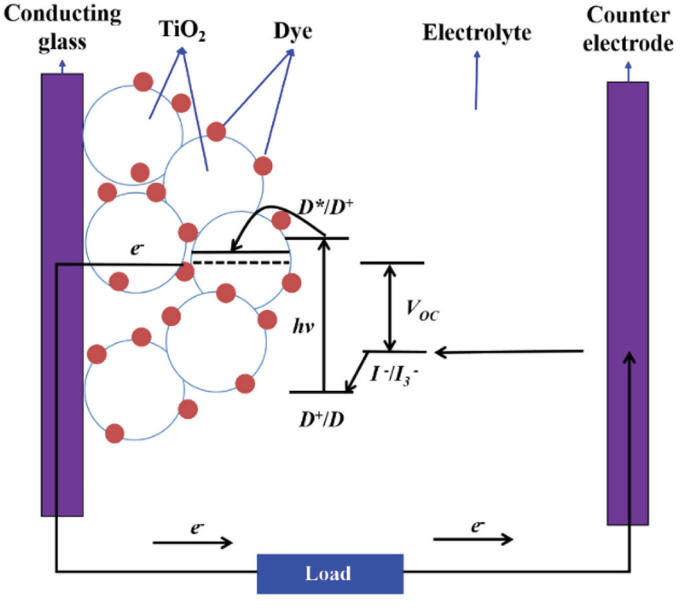

Figure 1. Schematic structure and working principle of a dye-sensitized solar cell.

2.2. Preparation of a DSSC

A DSSC was prepared as follows. Firstly, the FTO glass was patterned by laser scribing. The thickness of FTO was 2.2 mm. Secondly, the photoelectrode was prepared. Based on silk-screen printing, TiO_2 nanoparticle slurry with a size of 20 nm was prepared as the absorbed layer, and that with the sizes of 200 nm was prepared as the scattering layer. And then they were treated by 0.05 mol/L $TiCl_4$ solutions. Thirdly, the TiO_2 electrode was sensitized with cis-bis (iso-thiocyanato)-bis (2, 2′-bipyridyl-4, 4′-dicalboxylato) Ru (II) bis-tetrabutylammonium (N719). Fourthly, a Pt thin film was deposited on FTO by magnetron sputtering as the counter electrode. Fifthly, the liquid electrolyte was injected into the space between the anode and counter electrode. The liquid electrolyte consists of 0.6 M methylhexylimidazolium iodide, 0.05 M iodine, 0.1 M LiI and 0.5 M tert-butylpyridine in 3-methoxypropionitrile. Finally, a sandwich-like DSSC was assembled. Figure 2 shows the figure of DSSCs assembled. The whole thickness of the DSSC is 4.5 mm.

2.3. Experimental measurement

The maximum electron flux in outer space, that is earth radiation belt, is about $10^8/cm^2$ s. The energy range of electrons is 0.1–10 MeV. Given that the battery has the service life of 15 years, the total adsorbed dose of the DSSC is in the order of about kGy. Eighteen DSSC samples with similar initial performance before irradiation were used in the experiment. These DSSCs were exposed to 10 MeV electron irradiation at room temperature (25°C). The doses of electron irradiation were 0, 1, 2, 4, 8 and 10 kGy. The performances of FTO, semiconductor porous thin-film photoelectrode and dye sensitizer of DSSC were also researched and presented under electron irradiation.

J–V curves of DSSCs were measured by Keithley 2636A SourceMeter before and after electron irradiation at room temperature and standard illumination (Oriel, 94043A). The *J–V*

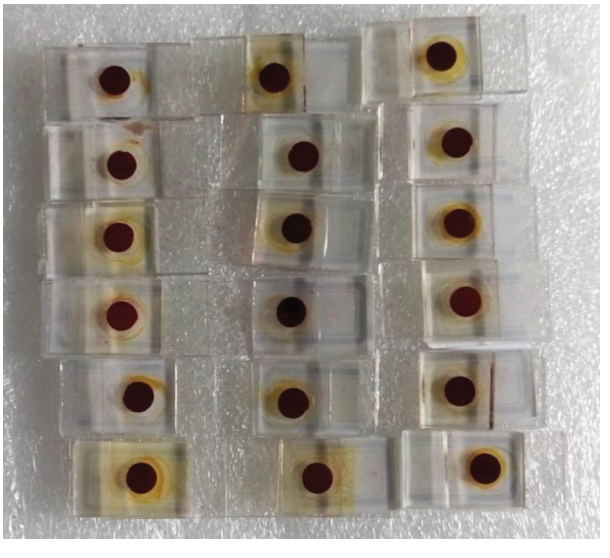

Figure 2. The photo of dye-sensitized solar cells assembled.

parameters refer to short-circuit current density (J_{sc}), open circuit voltage (V_{oc}), fill factor (*FF*) and the maximum output power (P_{max}). J_{sc} is the current through the DSSC when the voltage across the battery is zero. V_{oc} is the maximum voltage available from a DSSC and this occurs at zero current. P_{max} is the maximum value of the product of current and voltage. The values of *FF* is the ratio of P_{max} to the product of J_{sc} and V_{oc}.

The performances of FTO, dye sensitizer and anode were investigated before and after electron irradiation in detail. By using ultraviolet–visible spectrophotometer (Shimadzu, UV-2550), the transmission spectrum of FTO was measured in the scanning range of 300–900 nm. The absorption spectrum of dye molecules in anhydrous ethanol solution was also obtained with UV-2550. Then Fourier infrared spectrum (FT–IR) of dye molecules was studied by an online infrared-spectrum analyzer (Nexus, 670). Finally, X-ray diffraction (XRD) tests and Scanning Electron Microscope (SEM) tests were carried out to analyze the structure and the particle size of the anode. The size of the TiO_2 crystal was calculated according to the Scherrer Equation:

$$D_{hk1} = \frac{k\lambda}{U\cos\theta}, \tag{1}$$

where D_{hk1} is the grain size of the crystal on normal direction (hk1); k is the constant, 0.89; λ is the X-ray wavelength; θ is the diffraction angle; U is the difference between the measured width, that is full width at half maximum of the diffraction peak of the measured simple, and the instrument width, that is full width at half maximum of the diffraction peak of the standard simple.

3. Results and discussion

3.1. DSSC J–V characteristics with different electron irradiation doses

Figure 3 shows the changes in the normalized cell performance parameters as a function of electron dose. The 'normalized' values here means the values normalized to the value at the zero irradiation dose. The performance degradation of the solar cell parameters is

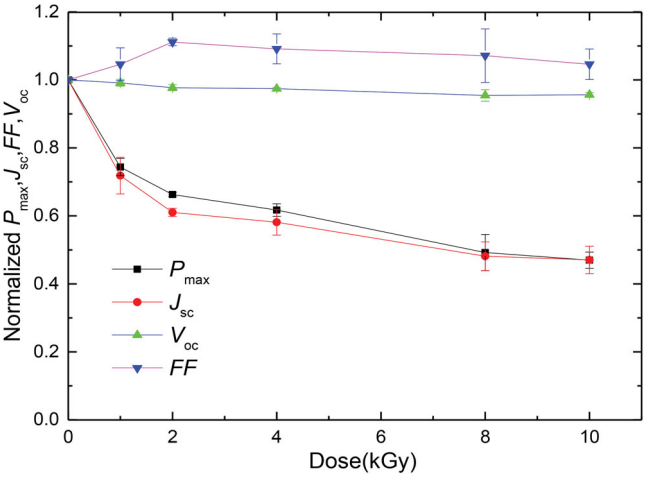

Figure 3. Normalized values of P_{max}, J_{sc}, *FF* and V_{oc} as a function of electron irradiation dose on DSSC.

dependent on the electron dose and the irradiation affects the solar cell parameters to a certain extent. The variations in V_{oc} or *FF* are not significant. After 10 kGy electron irradiation, the normalized value of V_{oc} is still 95%. However, the electron irradiation causes a large decrease in the J_{sc} and P_{max}. A sharp decrease in J_{sc} and P_{max} is observed on increasing the electron dose up to 10 kGy. Nearly 53% of the initial J_{sc} was decreased for the dose 10 kGy.

The value of P_{max} is sensitive to the value of J_{sc}. And the decreases in J_{sc} under electron irradiation may be related to the photocurrent in the DSSC. The photocurrent can be influenced by the performances of FTO, dye sensitizer and anode, which are three important parts of the DSSC. Therefore, the influences of electron irradiation on these three parts were studied as follows in detail. More explanations and analyses were given to support the decrease in J_{sc} and P_{max}, which follow.

3.2. The calculation of 10 MeV electron range

The range of electron over 2.5 MeV can be estimated using the following formula (*14*):

$$R = (530E_0 - 106)/1000\rho, \tag{2}$$

where R is the electron range (cm), E_0 is the electron energy (MeV), ρ is the material density (g/cm^3). According to Equation (2), the range of 10 MeV electron into FTO (For FTO, $\rho = 2.7$ g/cm^3) is 1.92 cm. The whole width of the DSSC device is 4.5 mm, so that the electron can easily get through the FTO into the cell. All part s of the DSSC could be affected by the electron. The effects of electron irradiation on FTO, dye sensitizer and anode were studied, to investigate the degradation of the DSSC, described below.

3.3. Influences of electron irradiation on FTO

Figure 4 shows the visible color-changing of FTO glasses under various electron irradiation doses. With increases in dose, the FTO glasses become more and more brown or black. Figure 5 shows the change in spectra response of FTO before and after electron irradiation. The non-irradiated FTO exhibits the highest transmittance in the whole wavelength range. The transmittance values for FTO decrease with the increase in the electron irradiation dose. A significant decrement is observed after electron irradiation in the range of 300–900 nm. The minimum value of transmittance for each curve occurs at 430 nm. Because of the absorption of photons in FTO, the transmittance values reduce dramatically. A constant degradation in the transmittance reduces the number of photons into the DSSC and decreases the value of photon current.

The electron irradiation induces external structural defects on FTO. These defects may destroy the stability of the potential field. The electronic energy state is changed and then the impurity energy level appears in the FTO semiconductor during electron irradiation. With the action of impurity energy level, the new absorption centers are created and lead to the transparent FTO coloring (*15*, *16*). Therefore, FTO turns brown or black after irradiation and then the light transmittance is reduced. The light absorption by FTO will reduce the number of incident photons to the DSSC markedly, which can decrease the value of J_{sc}.

In addition, the square resistances of FTO were measured by the four-point probe method (Guangzhou, RTS-8). Figure 6 indicates that the values of FTO square resistance are not significantly changed after electron irradiation. It can be concluded that the electron

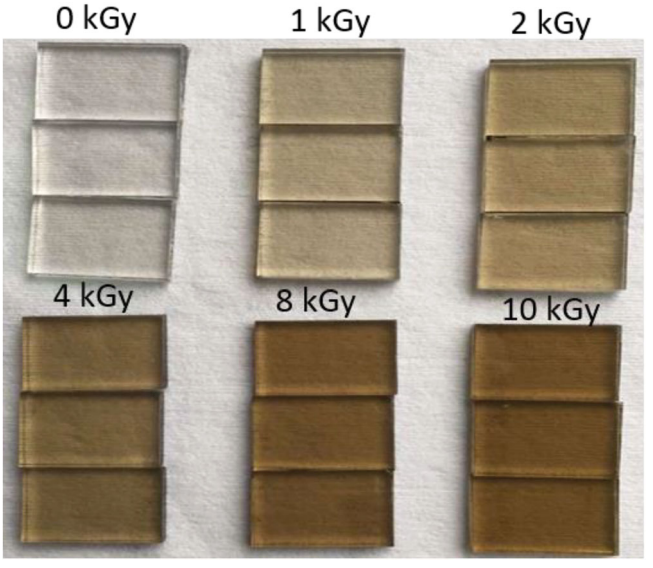

Figure 4. FTO glasses under various electron irradiation doses.

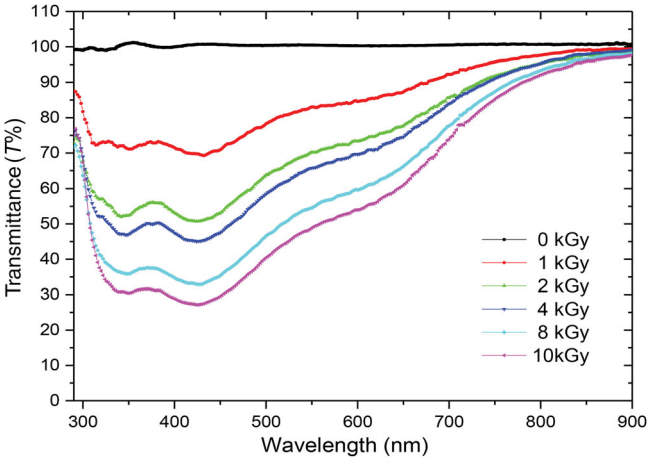

Figure 5. FTO transmission spectra response under various electron irradiation doses.

irradiation effect, like γ irradiation effect (*12*), on the conductivity of FTO is almost negligible. According to the analyses above and our previous study (ref (*12*)), it can be found that the influence of electron on FTO is similar to that of gamma.

3.4. Influences of electron irradiation on n719 dye

Figure 7 shows the molecular structure of N719 dye. N719 is the most widely used sensitizer in the DSSC. Under the interactions between the carboxyl groups in the dye and the surface of TiO_2, dye is absorbed on the surface of TiO_2 (*17*).

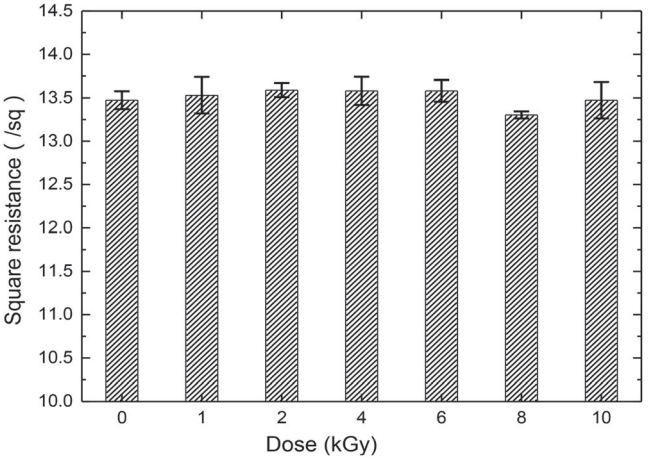

Figure 6. Square resistance of FTO under different electron irradiation doses.

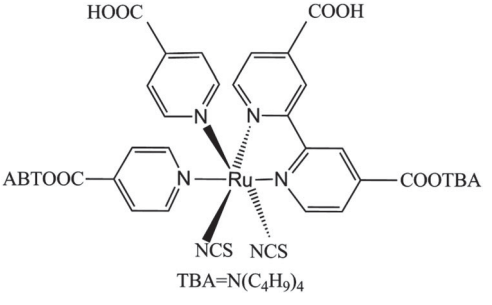

Figure 7. Molecular formula for N719 dye.

Figure 8 shows the typical UV–VIS absorption spectra of dye molecules as a function of electron irradiation dose in anhydrous ethanol solution. Three absorption peaks can be found obviously in Figure 8. With the increase of electron irradiation doses, dye molecules have slight loss of color. Three absorption peaks are observed from the absorption spectrum of N719 dye solution within the range of 300–900 nm. With the increase in the electron irradiation dose, the intensity of absorption peaks is decreased. The intensity of the absorption peaks will affect the absorption of photos of the chromophore group, weaken the absorption of light of dye and attenuate DSSC performance. The results are consistent with previous results (*12*, *18*, *19*).

High molecular materials, such as N719, are prone to fracture under radiation. This will lead to the degradation of molecular materials and affect the performance of the device. The absorption spectra of N719 dye molecules have changed after electron irradiation. The fracture of N719 dye contributes to this phenomenon. FT–IR can be used to analyze the change of chemical bonds for N719 dye. Figure 9 shows the flourier transform infrared spectra of N719 dye under different electron irradiation doses.

As shown in Figure 9, the four vibrational peaks at 1630, 1612, 1472, 1402 cm^{-1} on the pyridine ring of N719 molecules have not been changed after radiation. This result

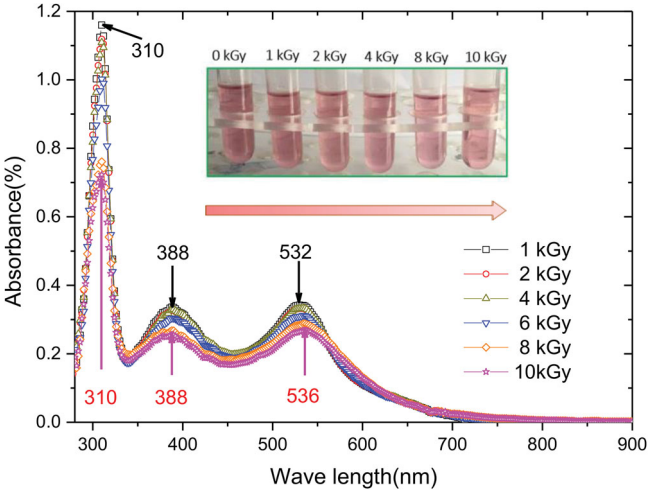

Figure 8. UV–VIS absorption spectra of N719 dye in anhydrous ethanol solution.

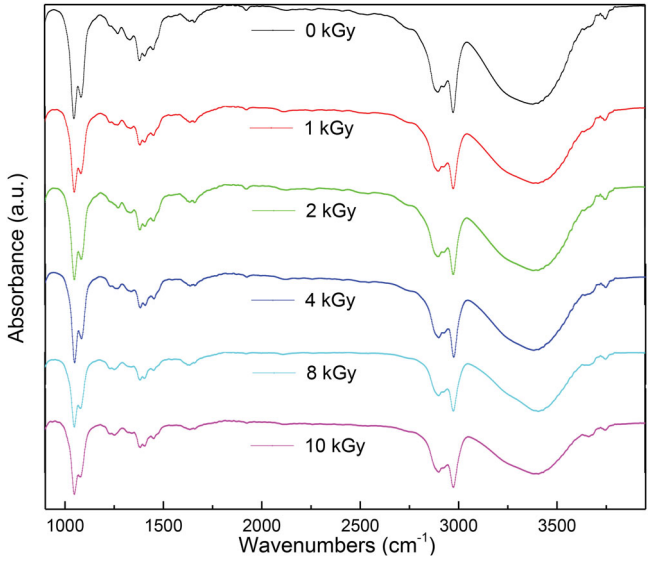

Figure 9. FT-IR of N719 dye under different electron irradiation doses.

states that the electron irradiation does not cause damage on the pyridine ring structure of dye molecules. There is also no obvious variation about the vibrational peaks at 2104 and 773 cm^{-1}, which are assigned to -CNS moieties in N719 molecular. However, the vibrational peak at 1233 cm^{-1}, which is assigned to –COOH moiety in N719 molecular, has been obviously changed after the electron irradiation. The vibrational peak value decreases as the increasing of electron doses. This result reveals that the –COOH moiety is ruptured due to the high electron irradiation dose. Figure 10 shows the interaction processes between dye N719 and electron irradiation. The structure of dye N719 has been changed because of the fracture of carboxyl at electron irradiation. The breaking of –COOH moiety for N719

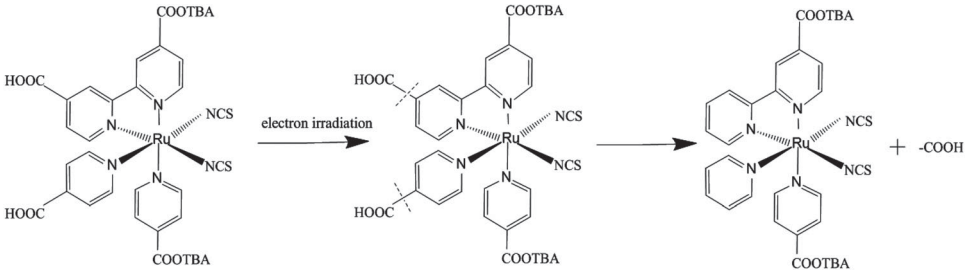

Figure 10. The interaction processes of electron irradiation and dye molecules.

dye could contribute to the decreasing of the intensity of absorption peaks, and then leads to the decreasing of the short-circuit current. On the other hand, the intermediates generated in TiO_2 or solvent by the electron irradiation also cause the damage of dye N719, and affect the short-circuit current of the DSSC. This is similar to the result under γ irradiation in ref (*12*).

However, as shown in Figure 8, absorption peaks have almost no red-shift or blue-shift for the three peaks with increase in doses. Only at the third absorption peak is there a little red-shift, from 532 to 536 nm. Under the harsh electron irradiation dose, that is 10 kGy, the orbital energy level of the dye molecule could have changed after irradiation. And this phenomenon may contribute to the red-shift.

3.5. Influences of electron irradiation on TiO_2 anode

The XRD measurement was carried out under 35 kV and 20 mA (Figure 11). Comparing the positions of peaks before and after electron irradiation, XRD spectra do not change obviously. The result shows that TiO_2 has not transformed from the anatase phase to the rutile phase. According to Equation (2), the crystal grain size in the normal direction of the (110)

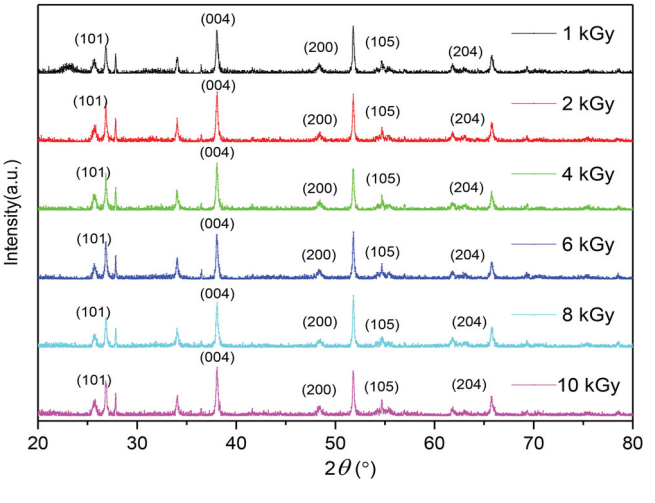

Figure 11. XRD measurement of TiO_2 anode under different electron irradiation doses.

was calculated. As shown in Figure 12, with the increase in the irradiation dose, the crystal grain size along the normal direction of the (110) firstly decreases, then increases and finally decreases. The results show that the grain size of TiO_2 changed by electron irradiation. This phenomenon caused by rupturing and formatting of Ti–O bond in TiO_2 crystallites under electron irradiation (*12, 20, 21*).

The absorption of dye molecules in the anode are closely related to the grain size of TiO_2. The smaller crystal size means the larger specific surface and the larger dye molecules absorbed in the anode. However, with the decrease in the grain size of TiO_2, the average pore diameter of the thin-film anode is decreased. If the average pore diameter is too small,

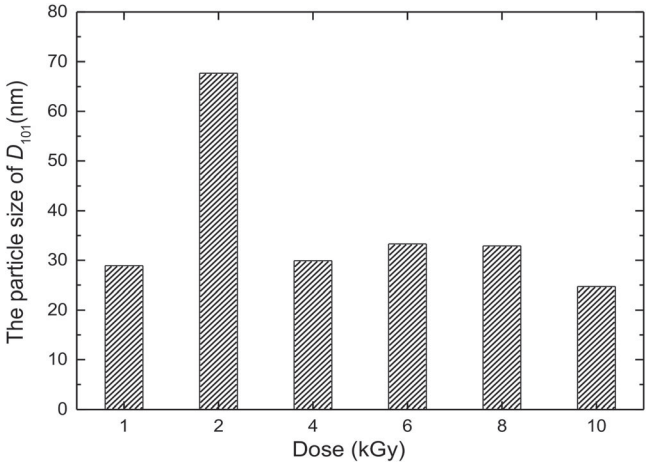

Figure 12. The grain size of TiO_2 under different electron irradiation doses.

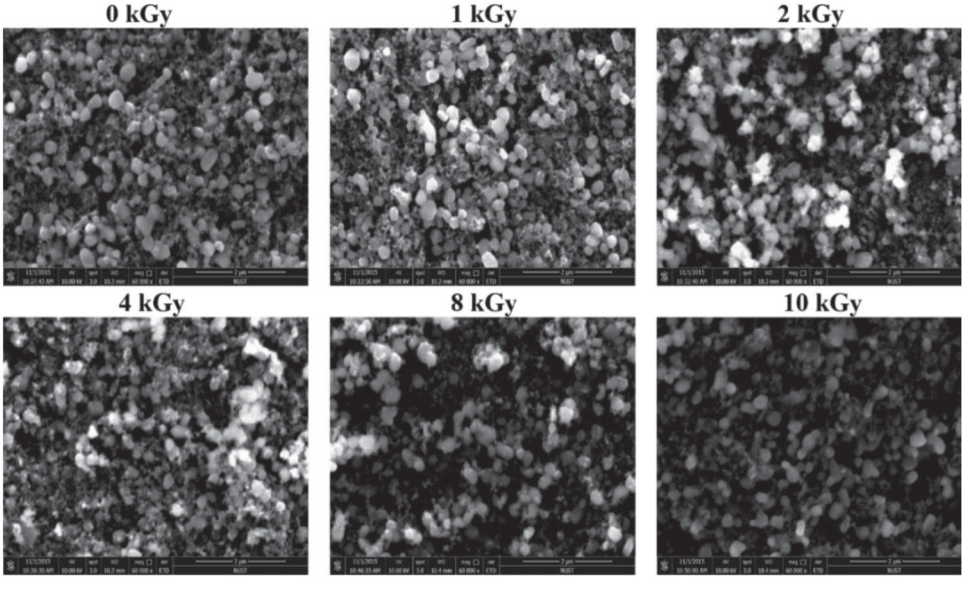

Figure 13. The surface of TiO_2 under different electron irradiation doses.

the dye molecules and electrolyte cannot enter TiO_2 effectively. As a result, the grain size if TiO_2 requires an optimal value to achieve maximum efficiency of the DSSC.

In order to study the variation of nanometer titanium dioxide surface before and after electron irradiation, the TiO_2 films are studied by SEM. As shown in Figure 13, there is a significant change in the surface morphology of TiO_2 after electron irradiation. The particles have distribute homogeneous before electron irradiation, and then the nanometer titanium dioxide appear agglomerate phenomena after electron irradiation. The conglomeration of nano-particles has much lower surface area. This is not good for the attachment of dye molecules on to TiO_2 which can decrease the value of J_{sc} and cause the fall of cell performance.

4. Conclusions

Through measuring the *J–V* curves of DSSC before and after irradiation, the effects of electron irradiation on the electrical properties of DSSC have been studied in this paper. To investigate the degradation of DSSC after irradiation, the electron irradiation effects on FTO, dye sensitizer and anode are studied. The following conclusions are drawn:

- The cell performance is significantly changed after the DSSC is exposed in electron irradiation. With the increase in the electron irradiation dose, J_{sc} and P_{max} of DSSC decrease significantly.
- The color centers are induced on FTO by electron irradiation. The phenomenon reduces the light transmittance of FTO and leads to the decrease of J_{sc}.
- The structure of the N719 dye molecule has been changed after electron irradiation. The phenomenon results in a blue-shift in the absorption spectra of dye molecules and then reduces the absorption of photons in the DSSC.
- Under 10 MeV electron irradiation, even for 10 kGy, the TiO_2 still has not transformed from the anatase phase to the rutile phase. However, the grain size and the surface morphology of TiO_2 are changed after electron irradiation, thus affecting the performance of the DSSC.

Disclosure statement

No potential conflict of interest was reported by the authors.

Funding

This work was supported by the National Natural Science Foundation of China [no. 11505096, 11675076], the National Defense Basic Scientific Research Project [no. JCKY2016605C006], the Natural Science Foundation of Jiangsu Province [no. BK20150735], the Shanghai Aerospace Science and Technology Innovation Fund, the Jiangsu Planned Projects for Postdoctoral Research Funds [grant no. 1601139B], the Priority Academic Program Development of Jiangsu Higher Education Institutions, and the Fundamental Research Funds for the Central Universities [no. NJ20160031].

References

(1) Xapsos, M.A.; O'Neill, P.M.; O'Brien, T.P. *IEEE Trans. Nucl. Sci.* **2013,** *60,* 1691–1705.

(2) Ginet, G.P.; O'Brien, T.P.; Huston, S.L.; Johnston, W.R.; Guild, T.B.; Friedel, R.; Lindstrom, C.D.; Roth, C.J.; Whelan, P.; Quinn, R.A.; Madden, D.; Morley, S.; Su, Y.-J. *Space Sci. Rev.* **2013,** *179* (1–4), 579–615.
(3) Schwank, J.R.; Shaneyfelt, M.R.; Dodd, P.E. *IEEE Trans. Nucl. Sci.* **2013,** *60* (3), 2074–2100.
(4) de Angelis, N.; Bourgoin, J.C.; Takamoto, T.; Khan, A.; Yamaguchi, M. *Sol. Energ. Mat. Sol. Cells.* **2001,** *66* (1), 495–500.
(5) Mbarki, M.; Sun, G.C.; Bourgoin, J.C. *Semicond. Sci. Technol.* **2004,** *19* (9), 1081–1085.
(6) Chou, H.T.; Tseng, K.C.; Hsu, H.C. *IEEE J. Photovolt.* **2016,** *6* (1), 211–216.
(7) O'Regan, B.; Grätzel, M. *Nature* **1991,** *353* (6346), 737–740.
(8) Bari, D.; Cester, A.; Wrachien, N.; Ciammaruchi, L.; Brown, T.M.; Reale, A.; Di Carlo, A.; Meneghesso, G. *IEEE J. Photovolt.* **2012,** *2* (1), 27–34.
(9) Yella, A.; Lee, H.W.; Tsao, H.N.; Yi, C.; Chandiran, A.K.; Nazeeruddin, M.K.; Diau, E.W.G.; Yeh, C.Y.; Zakeeruddin, S.M.; Gratzel, M. *Science* **2011,** *334* (6056), 629–634.
(10) Klein-Kedem, N.; Cahen, D.; Hodes, G. *Acc. Chem. Res.* **2016,** *49* (2), 347–354.
(11) Kim, S.H.; Noh, Y.J.; Kwon, S.N.; Kim, B.N.; Lee, B.C.; Yang, S.Y.; Jung, C.H.; Na, S.I. *J Ind. Eng. Chem.* **2015,** *26,* 210–213.
(12) Liu, M.; Tang, X.; Liu, Y.; Xu, Z.; Wang, H.; Fang, M.; Chen, D.J. *J. Radioanal. Nucl. Chem.* **2016,** *308* (2), 631–637.
(13) Ito, S.; Murakami, T.N.; Comte, P.; Liska, P.; Grätzel, C.; Nazeeruddin, M.K.; Grätzel, M. *Thin Solid Films* **2008,** *516* (14), 4613–4619.
(14) Katz, L.; Penfold, A.S. *Rev. Mod. Phys.* **1952,** *24* (1), 28–44.
(15) Mcgrath, B.; Schönbacher, H.; Van de Voorde, M. *Nucl. Instrum. Methods.* **1976,** *135* (1), 93–97.
(16) Yang, K.J.; Wang, T.S.; Zhang, G.F.; Peng, H.B.; Chen, L.; Zhang, L.M.; Li, C.X.; Tian, F.; Yuan, W. *Nucl. Instrum. Methods B.* **2013,** *307,* 541–544.
(17) Meyer, T.J.; Meyer, G.J.; Pfennig, B.W.; Schoonover, J.R.; Timpson, C.J.; Wall, J.F.; Kobusch, C.; Chen, X.H.; Peek, B.M. *Inorg. Chem.* **1994,** *33* (18), 3952–3964.
(18) Kim, H.J.; Lee, J.W.; Park, H.J. *Transactions of the Korean Nuclear Society autumn meeting*, **2012**.
(19) Nazeeruddin, M.K.; Amirnasr, M.; Comte, P.; Mackay, J.R.; McQuillan, A.J.; Houriet, R.; Grätzel, M. *Langmuir* **2000,** *16,* 8525–8528.
(20) Gui-ang, L.; Da, L.; Chang-wei, Z.; Wei, X.; Lian-quan, C. *Radiat. Eff. Def. Solids.* **2014,** *169* (4), 293–299.
(21) Kim, S.R.; Parvez, M.K.J. *J. Mater. Res.* **2011,** *26* (8), 1012–1017.